




OPEN

Glycosphingolipid GM3 prevents albuminuria and podocytopathy induced by anti-nephrin antibody

Nagako Kawashima^{1,7}[✉], Shokichi Naito^{1,7}, Hisatoshi Hanamatsu^{2,3}, Masaki Nagane⁴, Yasuo Takeuchi¹, Jun-ichi Furukawa^{2,5}, Norimasa Iwasaki², Tadashi Yamashita⁴ & Ken-ichi Nakayama⁶

Podocytopathy, which is characterized by injury to podocytes, frequently causes proteinuria or nephrotic syndrome. There is currently a paucity of effective therapeutic drugs to treat proteinuric kidney disease. Recent research suggests the possibility that glycosphingolipid GM3 maintains podocyte function by acting on various molecules including nephrin, but its mechanism of action remains unknown. Here, various analyses were performed to examine the potential relationship between GM3 and nephrin, and the function of GM3 in podocytes using podocytopathy mice, GM3 synthase gene knockout mice, and nephrin injury cells. Reduced amounts of GM3 and nephrin were observed in podocytopathy mice. Intriguingly, this reduction of GM3 and nephrin, as well as albuminuria, were inhibited by administration of valproic acid. However, when the same experiment was performed using GM3 synthase gene knockout mice, valproic acid administration did not inhibit albuminuria. Equivalent results were obtained in model cells. These findings indicate that GM3 acts with nephrin in a collaborative manner in the cell membrane. Taken together, elevated levels of GM3 stabilize nephrin, which is a key molecule of the slit diaphragm, by enhancing the environment of the cell membrane and preventing albuminuria. This study provides novel insight into new drug discovery, which may offer a new therapy for kidney disease with albuminuria.

Podocyte injury may lead to podocytopathies, represented as either minimal change disease (MCD) or focal segmental glomerulosclerosis (FSGS)¹. Moreover, podocyte detachment has been documented in many proteinuric diseases and this damage is permanent because podocytes are terminally differentiated. Therefore, it is crucial to preserve the number/quality of podocyte cells to prevent or inhibit the progression of podocytopathies.

Recently, there have been several reports concerning the function of glycosphingolipids in glomeruli² that suggest glycosphingolipid GM3 (Neu5Aca2,3Galβ1,4Glcβ1,1Cer) may be co-localized with nephrin in normal podocytes³, and possibly associated with vascular endothelial cell growth factor⁴. In addition, we have found that both MCD and FSGS patients had decreased GM3 and nephrin expression compared with healthy subjects, and in both MCD and FSGS patients, GM3 expression was negatively correlated with proteinuria⁵. However, the relationship between GM3 and glomerular function, especially in terms of podocytes, remains unclear². Glycosphingolipids, which make up part of the cell membrane, are important in transduction and regulation of various extracellular stimuli with intracellular activities⁶. For example, glycosphingolipid GM3 in squamous cell carcinoma and glioblastoma regulates several receptors (e.g. epidermal growth factor receptor, insulin receptor). Interaction of a receptor with GM3 can lead to inhibition of receptor signaling at the cell membrane, resulting in suppression of cellular proliferation^{7–10}. Excessive accumulation of glycosphingolipid in the lysosome membrane results in abnormal intracellular signaling^{11,12}. Indeed, overexpressed glycosphingolipid on the cell membrane modulates membrane protein function^{10,13}.

¹Department of Nephrology, School of Medicine, Kitasato University, 1-15-1 Kitasato, Minami, Sagami-hara, Kanagawa 252-0374, Japan. ²Department of Advanced Clinical Glycobiology, Faculty of Medicine and Graduate School of Medicine, Hokkaido University, Kita15jyo - Nishi7chome, Kita, Sapporo, Hokkaido 060-8638, Japan. ³Department of Gastroenterology and Hepatology, Graduate School of Medicine, Hokkaido University, Kita15jyo-Nishi7chome, Kita, Sapporo, Hokkaido 060-8638, Japan. ⁴Biochemistry, School of Veterinary Medicine, Azabu University, 1-17-71 Fuchinobe, Chuo, Sagami-hara, Kanagawa 252-5201, Japan. ⁵Institute for Glyco-Core Research (iGCORE), Nagoya University, 65 Tsurumai, Showa, Nagoya, Aichi 466-8550, Japan. ⁶National Institute of Advanced Industrial Science and Technology (AIST), 1-1-1 Umezono, Tsukuba, Ibaraki 305-8560, Japan. ⁷These authors contributed equally: Nagako Kawashima and Shokichi Naito. ✉email: nagacok@kitasato-u.ac.jp

Several studies have reported on the therapeutic effect of valproic acid (VPA) for albuminuria^{14,15}. Moreover, VPA is known as an up-regulator of GM3 synthase gene (*ST3GAL5*; CMP-NeuAc:lactosylceramide α 2,3-sialyltransferase; EC2.4.99.9) that increases the level of glycosphingolipid GM3^{13,16,17}. Therefore, we reasoned that VPA may help alleviate kidney disease by causing increased expression of GM3. To demonstrate the above, we performed experiments using podocytopathy mice that showed the administration of VPA had a preventive effect on kidney disease. In order to examine the importance of GM3, the same experiment was performed using GM3 synthase gene knockout mice. Furthermore, Watts et al. recently reported that anti-nephrin antibodies are implicated in MCD patients¹⁸, a disease which at least some degree resembles to the phenotype of anti-Nphs Ab-induced podocytopathy mice in this study.

In this study, we examined whether albuminuria, glomerulosclerosis and podocyte foot process effacement were inhibited by elevated levels of GM3 brought about by administration of VPA using anti-nephrin antibody (anti-Nphs Ab)-induced podocytopathy mice¹⁹. These findings suggest up-regulation of *ST3GAL5* is effective as a novel therapeutic and preventive strategy for kidney disease with podocytopathy.

Results

Expression of nephrin and GM3 in mouse glomeruli. Our results showed both nephrin and GM3 were expressed in glomeruli of normal mouse kidney (Fig. 1A,B). However, by the 7 day after administration with 1.5 mg of anti-Nphs Ab, levels of nephrin and GM3 were drastically decreased (Fig. 1B). The podocyte foot processes in vehicle mice were normal. By contrast, podocyte foot process effacement (FPE) was evident only 3 hrs after anti-Nphs Ab injection (Fig. 1C,D). These results suggest that GM3 cooperates with nephrin and that this might be related to podocytopathy.

Preventive effect of podocytopathy by GM3 via administration of VPA. We previously reported that VPA can up-regulate and enhance GM3 expression via *ST3GAL5* induction^{13,16,17}. Therefore, we reasoned that enhanced GM3 expression induced by VPA might prevent anti-Nphs Ab-induced podocytopathy brought on by administration of 1.5 mg anti-Nphs Ab. To demonstrate whether GM3 can ameliorate podocytopathy, prevention tests with VPA were performed using mice displaying podocytopathy (Fig. 2A). Although there was no significant difference between blood urea nitrogen (BUN) and serum albumin levels, albuminuria levels were clearly different in VPA + podocytopathy mice compared with podocytopathy mice (Fig. 2B–D). The number of p57-positive cells (podocytes) decreased, and glomerulosclerosis increased in podocytopathy mice, compared with control. However, the number of podocytes and glomerulosclerosis were improved in VPA + podocytopathy mice (Fig. 2E–H). Nephrin and GM3 were clearly decreased in the glomeruli of podocytopathy mice, compared with control mice on day 1, 7, 14 after anti-Nphs Ab injection (Fig. 2I–K, Supplementary Fig. S1). Especially, GM3 was barely detectable on day 1 after anti-Nphs Ab injection, when albuminuria was most prevalent (Fig. 2G, Supplementary Fig. S1F). However, levels of nephrin and GM3 in the glomeruli of VPA + podocytopathy mice were almost the same as the control. GM3 expression was more enhanced in VPA administered mice compared with control. Moreover, FPE in podocytopathy mice were significantly blocked by VPA pre-administration (Fig. 2L,M). These results clearly demonstrate that elevated levels of GM3 brought about by administration of VPA had a preventive effect on anti-Nphs Ab-induced podocytopathy.

Disruption of GM3 synthase gene (*St3gal5*^{-/-}) induced podocytopathy. We identified albuminuria that occurred in 33 week-old *St3gal5*^{-/-} mice (Fig. 3A). The glomeruli of *St3gal5*^{-/-} mice had reduced numbers of podocytes (Fig. 3B,C). In 33 week-old *St3gal5*^{-/-} mice, the expression of nephrin also tended to decrease (Fig. 3D–F). Moreover, *St3gal5*^{-/-} mice had glomerular hypertrophy compared with *St3gal5*^{+/+} mice. FPE was observed in the kidneys of 33 week-old *St3gal5*^{-/-} mice (Fig. 3G,H), suggesting these mice showed podocytopathy. Next, prevention tests with VPA were performed using 13 week-old *St3gal5*^{-/-} mice administered with 1.5 mg of anti-Nphs Ab, equivalent to mice shown in Fig. 2A (Fig. 4A). The *St3gal5*^{-/-} mice showed markedly enhanced sensitivity to anti-Nphs Ab injury. Specifically, administration of VPA did not inhibit albuminuria (Fig. 4B–D) and the appearance of podocyte detachment and sclerotic lesions (Fig. 4E–H) in podocytopathy and VPA + podocytopathy *St3gal5*^{-/-} mice. In addition, immunofluorescence staining of 13 week-old *St3gal5*^{-/-} mice clearly showed the level of nephrin was reduced after administration of anti-Nphs Ab. Moreover, even if VPA was pre-administered, nephrin injury caused by anti-Nphs Ab could not be prevented (Fig. 4I–K). These results suggest that the effect of VPA was to act as a histone deacetylase (HDAC) inhibitor except increase of GM3 expression via *ST3GAL5* upregulation did not inhibit podocytopathy. Hence, GM3 is essential for glomerular maintenance (Figs. 2, 3, 4, Supplementary Fig. S1).

Effect of anti-nephrin antibody and VPA on nephrin injury in model cells. To investigate whether nephrin injury could be prevented by elevated levels of GM3 via administration of VPA using podocytes and HEK293/Nephrin (HEK/Nphs) cells. The expression of GM3, nephrin and F-actin bundle assembly as an indicator of healthy cells were compared under various treatment conditions (Fig. 5A,B, Supplementary Fig. S3A). As a result, after anti-Nphs Ab treatment GM3 was barely detectable and the levels of nephrin and F-actin bundle assembly were decreased. However, VPA treatment elicited an increase in the level of nephrin, GM3 and F-actin bundle assembly despite anti-Nphs Ab treatment (Fig. 5A,B, Supplementary Fig. S3A). Immunocytochemistry also indicated a correlation with anti-Nphs Ab-induced podocytopathy mice. Next, we examined VPA specificity for enhancement of GM3 expression in glycosphingolipid biosynthesis via induction of *ST3GAL5*. Exhaustive analysis of the expression of all glycosphingolipid-glycans in HEK/Nphs cells was performed using Glycoblots and Tandem-MALDI-TOF/MS^{20–23} (Supplementary Fig. S4A–C). The molecular species were analyzed and quantified using various treated HEK/Nphs cells. The amount of total ganglio-series of gangliosides (Gg),

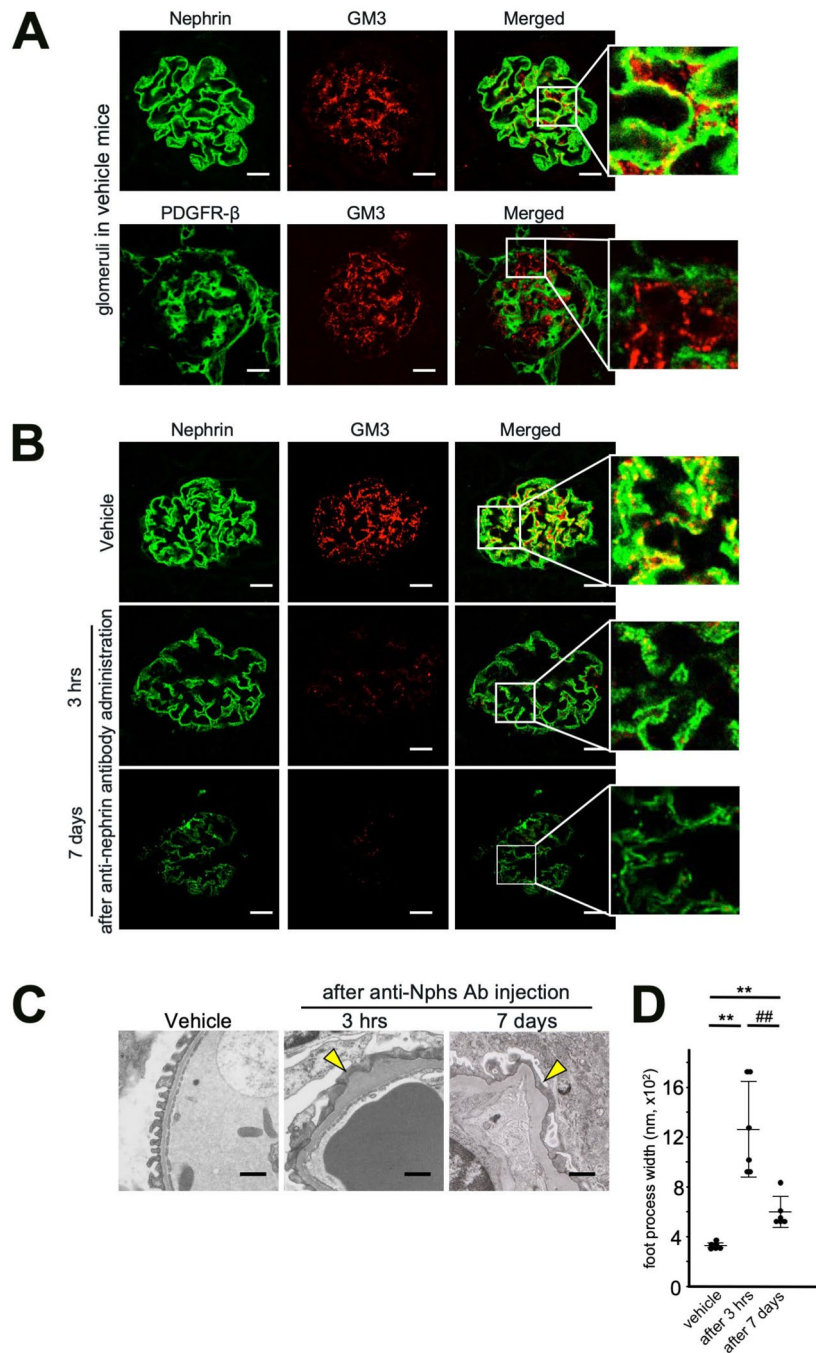


Figure 1. Localization of Nephrin, PDGFR- β and GM3 in glomeruli and the effect of anti-nephrin antibody on the podocyte foot process. **(A)** Immunofluorescence staining images of glomeruli in vehicle mice. Nephrin, or PDGFR- β and GM3 merged fluorescence images of the glomeruli of vehicle mice. Scale bars: 20 μ m. Nephrin (green), or PDGFR- β (green) and GM3 (red) merged areas (yellow) highlighted in enlarged images. **(B)** Immunofluorescence staining images of glomeruli in 1.5 mg of anti-nephrin antibody (anti-Nphs Ab)-induced podocytopathy mice. Scale bars: 20 μ m. Nephrin (green) and GM3 (red) merged areas (yellow) highlighted in enlarged images. **(C)** Transmission electron microscopy images of podocyte foot processes in vehicle mice and anti-Nphs Ab-induced podocytopathy mice. Yellow arrowheads showing areas of foot process effacement. Scale bars: 10 μ m. **(D)** Scatter diagram showing quantification of foot process effacement. $**P < 0.01$ vs. vehicle, $##P < 0.01$ vs. 3 h after antibody administration. Statistical analyses were performed from mice ($n = 6$) in each group.

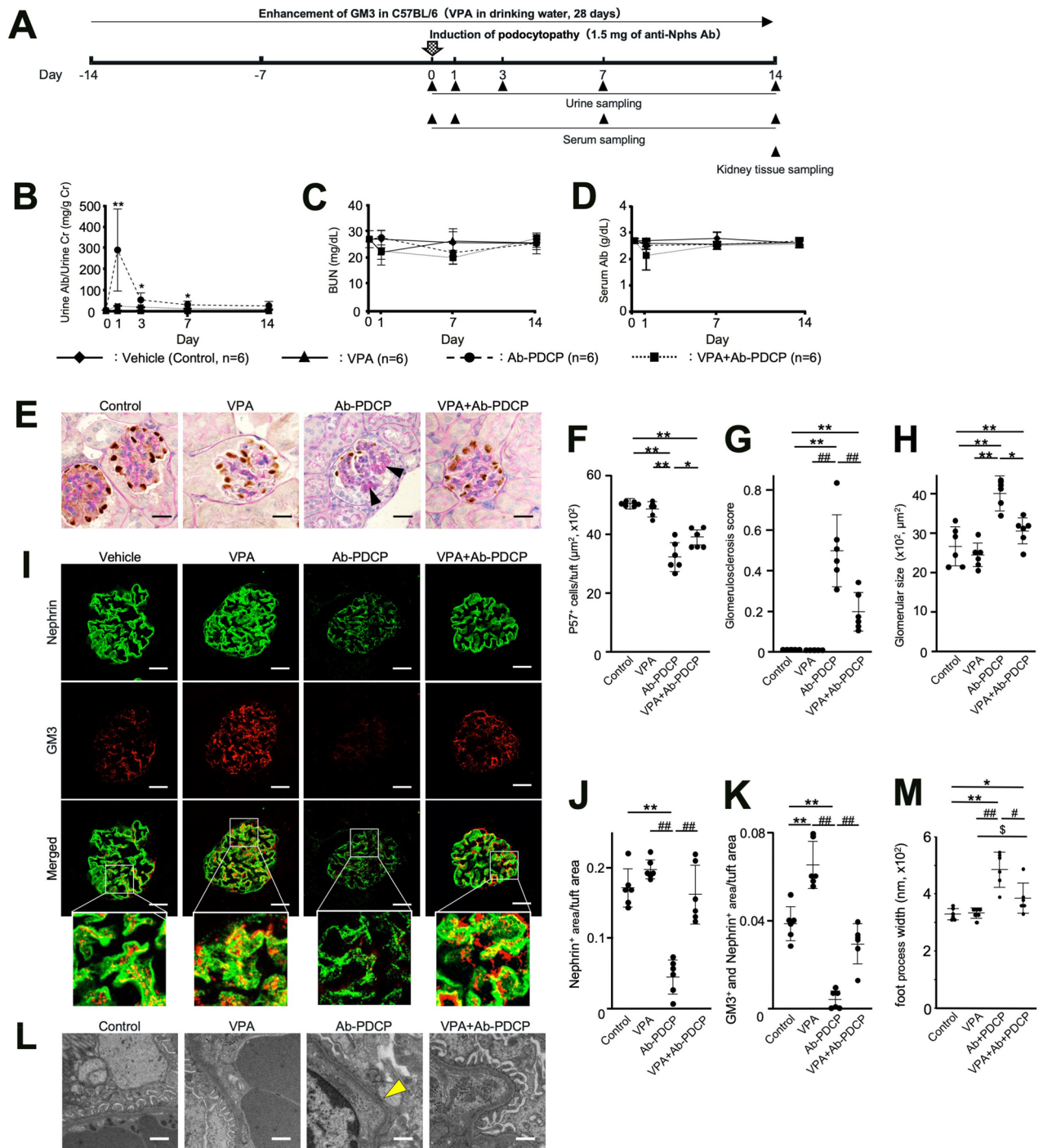


Figure 2. Preventive effect of podocytopathy by GM3 via administration of VPA in anti-nephrin antibody-induced podocytopathy mice. **(A)** Schedule for podocytopathy prevention test using VPA. **(B)** Line graph showing urine albumin to creatinine, **(C)** urea nitrogen (BUN), **(D)** serum albumin. Vehicle (Control), VPA administered mice (VPA), 1.5 mg of anti-nephrin antibody (anti-Nphs Ab)-induced podocytopathy (Ab-PDCP), and VPA + 1.5 mg of anti-Nphs Ab-induced podocytopathy (VPA + Ab-PDCP) mice are shown as a solid line with diamond, a solid line with triangle, dashed line with circle and dotted line with square, respectively. * $P < 0.05$; ** $P < 0.01$ vs. control. **(E)** p57 (podocyte marker, brown) and periodic acid-Schiff (PAS) staining of glomeruli. Arrowhead showing glomerulosclerosis. Scale bars: 20 μm . **(F)** Scatter diagram showing p57 + cells/tuft, **(G)** glomerulosclerosis score, and **(H)** glomerular size, respectively. Twenty glomeruli per mouse were analyzed in each dot. * $P < 0.05$; ** $P < 0.01$ vs. control, ## $P < 0.01$ vs. Ab-PDCP. **(I)** Immunofluorescence staining images of glomeruli. Scale bars: 20 μm . Nephrin (green) and GM3 (red) merged areas (yellow) highlighted in enlarged images. **(J)** Scatter diagram showing nephrin fluorescence area/tuft area, **(K)** GM3 and nephrin merged fluorescence area/tuft area. ** $P < 0.01$ vs. control, ## $P < 0.01$ vs. Ab-PDCP. **(L)** Images of podocyte foot processes by transmission electron microscopy. Yellow arrowhead showing area of foot process effacement. Scale bars: 10 μm . **(M)** Scatter diagram showing quantification of foot process effacement. * $P < 0.05$; ** $P < 0.01$ vs. control, # $P < 0.05$; ## $P < 0.01$ vs. Ab-PDCP, \$ $P < 0.05$ vs. VPA. Statistical analyses were performed from mice ($n = 6$) in each group.

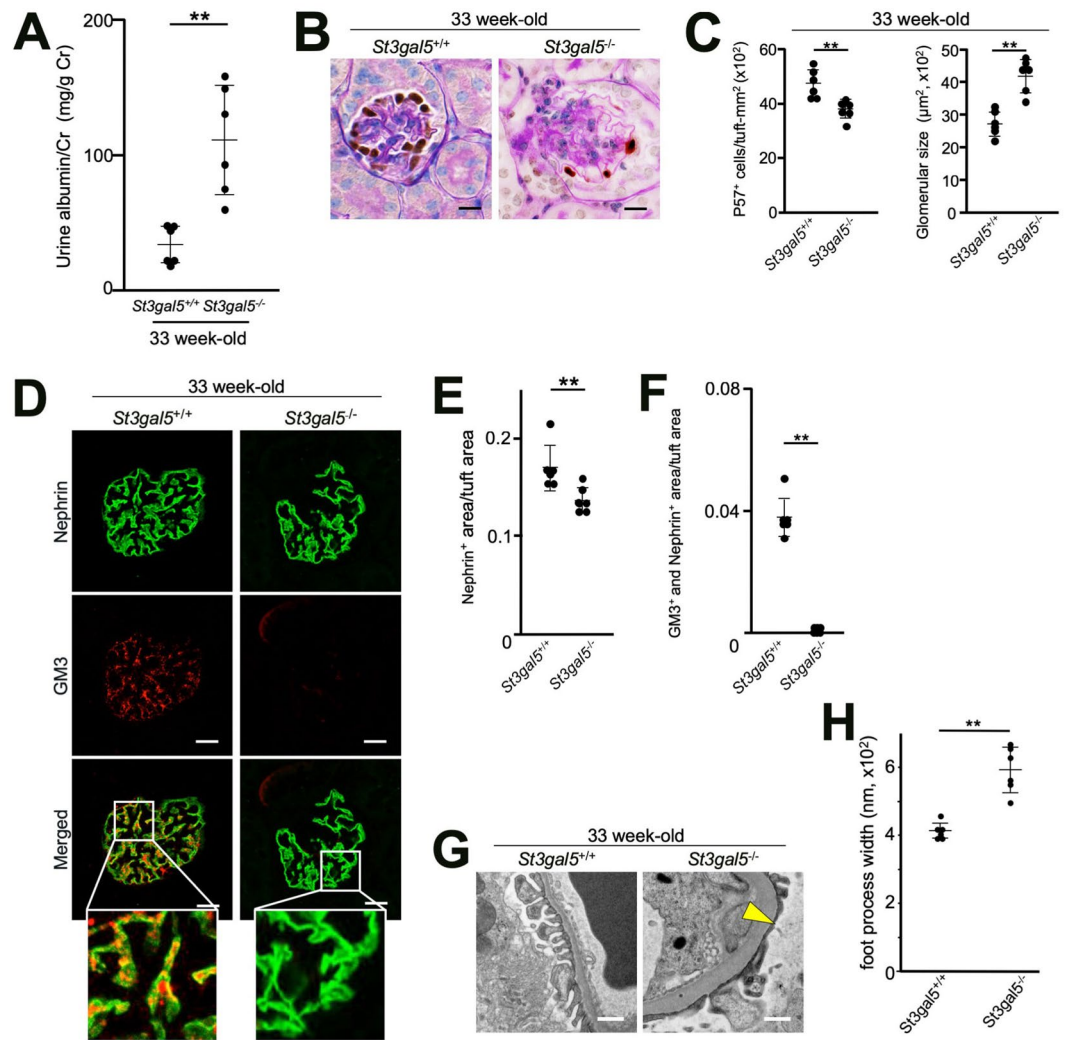


Figure 3. Podocytopathy in aged GM3 synthase gene knockout (*St3gal5*^{-/-}) mice. **(A)** Scatter diagram showing urine albumin to creatinine. ***P* < 0.01 vs. wild-type (*St3gal5*^{+/+}) mice. **(B)** p57 (podocyte marker, brown) and PAS staining of glomeruli. Scale bars: 20 µm. **(C)** Bar graphs showing p57 + cells/tuft (left) and glomerular size (right). ***P* < 0.01 vs. *St3gal5*^{+/+}. **(D)** Immunofluorescence staining images of glomeruli. Scale bars: 20 µm. Nephryn (green) and GM3 (red) merged areas (yellow) highlighted in enlarged images. **(E)** Scatter diagram showing nephryn fluorescence area/tuft area, **(F)** GM3 and nephryn merged fluorescence area/tuft area. ***P* < 0.01 vs. *St3gal5*^{+/+}. **(G)** Images of podocyte foot processes by transmission electron microscopy. Yellow arrowhead showing areas of foot process effacement. Scale bars: 10 µm. **(H)** Scatter diagram showing quantification of foot process effacement. ***P* < 0.01 vs. *St3gal5*^{+/+}. Twenty glomeruli per mouse were analyzed in each group. Statistical analyses were performed from mice (*n* = 6) in each group.

especially GM3 (Neu5Acα2,3Galβ1,4Glc), in anti-Nphs Ab treated cells decreased compared with untreated cells. By contrast, VPA + anti-Nphs Ab treated cells displayed an increase in the amount of total Gg expression compared to untreated cells. Thus, VPA treatment elicited an increase in the level of total Gg, especially GM3 (Neu5Acα2,3Galβ1,4Glc), even though the cells were treated with anti-Nphs Ab at the same time. There was, however, no significant change in the levels of Gg except for GM3, lacto-series of gangliosides (Lc) and total globo-series of gangliosides (Gb) under the various treatment conditions. Thus, induction of *ST3GAL5* by VPA specifically enhanced GM3 expression and did not affect the level of other glycosphingolipids at the cell membrane as observed from in vivo and in vitro analyses (Figs. 2, 5, Supplementary Table S2, Supplementary Figs. S1–S4).

Interaction of nephryn and GM3 and their localization in the cell membrane. The immunoprecipitation results using podocytes and HEK/Nphs cells showed GM3 interacted with nephryn in untreated cells (Fig. 5C, Supplementary Fig. S3B). Moreover, the amount of nephryn decreased in anti-Nphs Ab treated cells. By contrast, nephryn levels were maintained in VPA + anti-Nphs Ab treated cells. This finding indicated nephryn interacts with GM3.

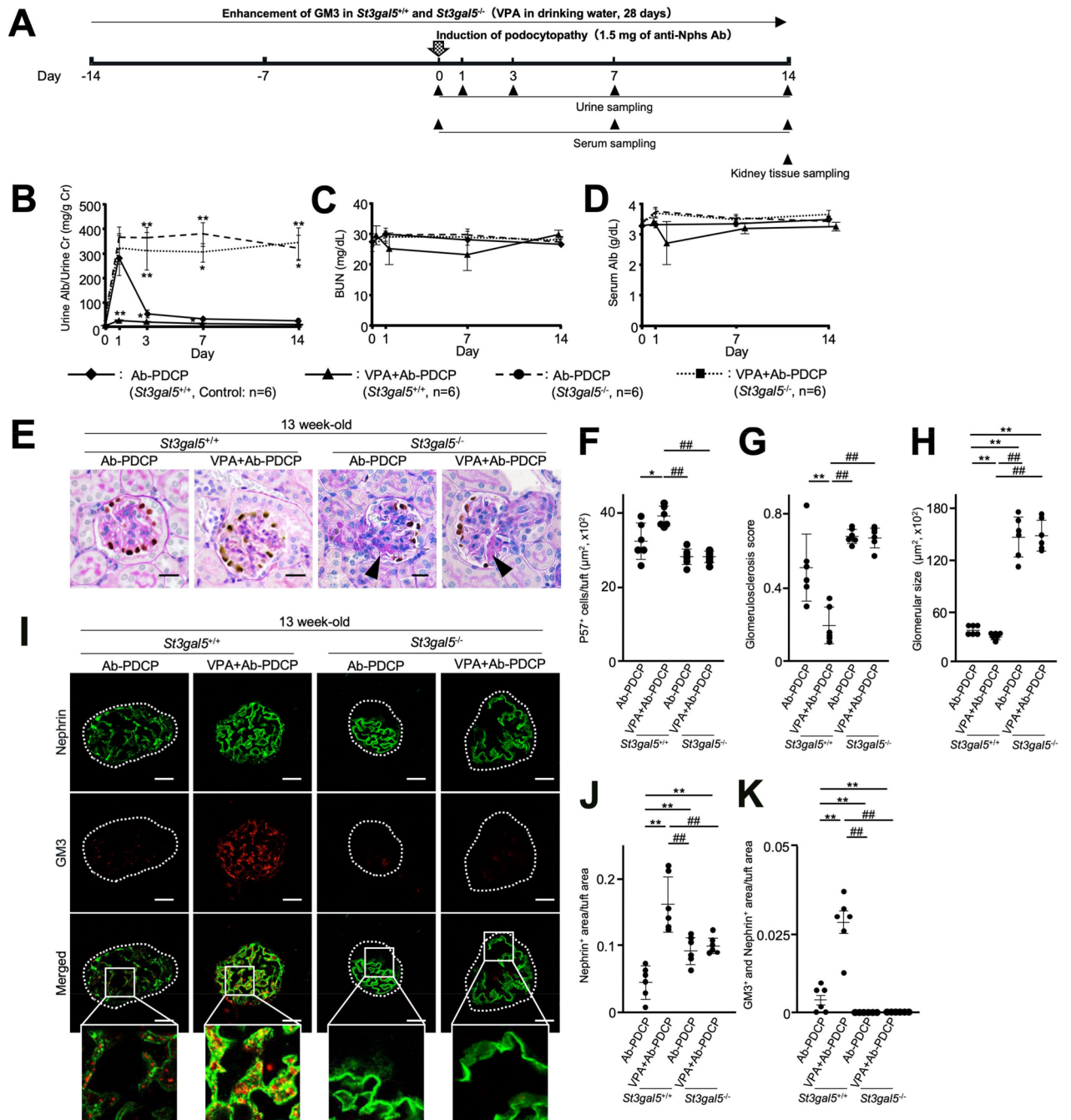


Figure 4. No preventive effect by administration of VPA in young GM3 synthase gene knockout (*St3gal5^{-/-}*) mice. **(A)** Schedule for podocytopathy prevention test using VPA. **(B)** Line graph showing urine albumin to creatinine, **(C)** urea nitrogen (BUN), **(D)** serum albumin (c). 1.5 mg of anti-nephrit antibody (anti-Nphs Ab)-induced podocytopathy (Ab-PDCP), and VPA + 1.5 mg of anti-Nphs Ab-induced podocytopathy (VPA + Ab-PDCP) in *St3gal5^{+/+}* and *St3gal5^{-/-}* mice are shown as a solid line with diamond, a solid line with triangle, dashed line with circle and dotted line with square, respectively. **P* < 0.05; ***P* < 0.01 vs. *St3gal5^{+/+}*. **(E)** p57 (podocyte marker, brown) and PAS staining of glomeruli. Arrowhead showing glomerulosclerosis. Scale bars: 20 μm. **(F)** Scatter diagram showing p57 + cells/tuft, **(G)** glomerulosclerosis score, and **(H)** glomerular size, respectively. Twenty glomeruli per mouse were analyzed in each dot. **P* < 0.05; ***P* < 0.01 vs. Ab-PDCP in *St3gal5^{+/+}*, #*P* < 0.01 vs. VPA + Ab-PDCP in *St3gal5^{+/+}*. **(I)** Immunofluorescence staining images of glomeruli. Scale bars: 20 μm. Nephrin (green) and GM3 (red) merged areas (yellow) highlighted in enlarged images. **(J)** Scatter diagram showing nephrin (green) fluorescence area/tuft area, **(K)** GM3 (red) and nephrin (green) merged fluorescence area/tuft area. ***P* < 0.01 vs. Ab-PDCP in *St3gal5^{+/+}*, #*P* < 0.01 vs. VPA + Ab-PDCP in *St3gal5^{+/+}*. Statistical analyses were performed from mice (n = 6) in each group.

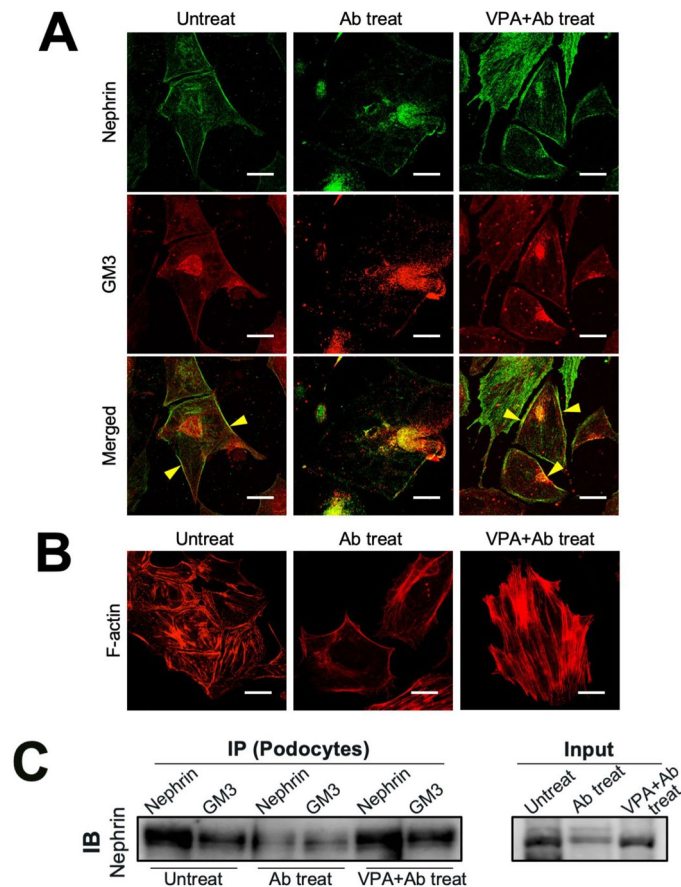


Figure 5. Effect of anti-nephrin antibody and VPA on podocytes and interaction of nephrin and GM3. **(A)** Immunofluorescence staining images of nephrin (green) and GM3 (red) in various treated podocytes. Yellow arrowheads showing merged areas of nephrin (green) and GM3 (red). **(B)** Immunofluorescence staining images of F-actin (red) in the same treated cells as A. Scale bars: 10 μ m. Untreated (Untreat), anti-Nphs Ab treated (Ab treat), preVPA + anti-Nphs Ab treated (VPA + Ab treat) podocytes. **(C)** Immunoprecipitation (IP) using cell lysate of various treated podocytes and anti-nephrin and GM3 antibodies, and immunoblot (IB) analysis using anti-Nphs antibody. Cell lysate of untreated (Untreat), anti-Nphs Ab treated (Ab treat), preVPA + anti-Nphs Ab treated (VPA + Ab treat) podocytes.

We investigated whether escape from nephrin injury by enhanced GM3 expression was due to interaction between nephrin and GM3. Nephrin and Fyn, which were originally localized in raft fractions (fraction 1–3; Glycolipid enriched membrane (GEM)), mostly shifted to non-raft fractions (fraction 4–10; non-GEM) after anti-Nphs Ab treatment (Supplementary Fig. S4D,E). In addition, caveolin-1 (a raft marker) also shifted in the same manner as nephrin. However, nephrin, Fyn and caveolin-1 were restored in the raft fractions by VPA treatment even though the cells were treated with anti-Nphs Ab. As observed with the shift of nephrin, GM3 tended to shift from raft fractions to non-raft fractions upon anti-Nphs Ab treatment (Supplementary Fig. S4F,G). Nonetheless, despite anti-Nphs Ab treatment, GM3 was restored to the raft fractions by VPA treatment to give a distribution akin to that seen for untreated cells. These results indicated that under normal conditions nephrin, GM3, Fyn and caveolin-1 were all localized in raft fractions. However, under abnormal membrane conditions, such as when anti-Nphs Ab interacts with nephrin, raft fractions were disordered and nephrin, GM3, Fyn and caveolin-1 shifted to non-raft fractions. Thus, these experiments also indicated that nephrin was able to escape injury induced by various extracellular factors via enhanced levels of GM3.

Discussion

The important finding to emerge from this study was that glycosphingolipid GM3 can be used to prevent albuminuria. Of particular importance is the preventive effect observed when GM3 was given to mice with podocytopathy.

We found that GM3 levels decreased together with nephrin in glomeruli of a podocytopathy mouse model induced by administration of anti-Nphs Ab (Fig. 1). Recently, the relationship between GM3 and maintenance of the slit diaphragm in podocytes as well as GM3 and cell adhesion has been reported^{14,24}. Here, we demonstrated the preventive effect of GM3 in anti-Nphs Ab-induced podocytopathy mice (Fig. 2) occurs via a newly identified mechanism involving GM3 enhancement induced by VPA^{13,16,17}. Specifically, we found that induction of sufficient

GM3 in podocyte cell membranes stabilized the slit diaphragm components, including nephrin (Fig. 5). The overall effect of GM3 induction was to inhibit podocyte detachment (Figs. 2, 3, 4, 5, Supplementary Figs. S1–S4). Moreover, we performed VPA preventive tests of podocytopathy induced by administration of anti-Nphs Ab using *St3gal5*^{-/-} mice (Fig. 4). Originally, *St3gal5*^{-/-} mice were established to investigate the relationship between GM3 and insulin resistance²⁵. Here, for the first time, we focused on the effect of GM3 on kidney (Figs. 3, 4). From our examinations, the following results were established. In young *St3gal5*^{-/-} mice (13 week-old) there were no significant differences in nephrin expression by comparison to wild-type mice (Fig. 3). Nonetheless, *St3gal5*^{-/-} mice showed podocytopathy with irreversible albuminuria by anti-Nphs Ab administration.

Furthermore, in young *St3gal5*^{-/-} mice (13 week-old), there were only very minor changes in the glomeruli (Supplementary Fig. S2). However, the loss of podocytes is not reflected in obvious symptoms. Thus, kidney function of these mice is maintained by components other than glycolipids (cholesterol, tetraspanin etc.)²⁶. Nonetheless, once positively stimulated by anti-Nphs Ab, there is a transition to an irreversible and severe disorder. It should be noted that proteinuria and sclerotic lesions appear even under unstimulated conditions in 33 week-old mice, unlike young mice. This effect presumably arises from factors associated with aging. It is likely that in the absence of GM3 other molecules participate in incomplete raft formation to maintain kidney function in *St3gal5*^{-/-} mice. In this study, using *St3gal5*^{-/-} mice, we found that incomplete rafts cannot recover from albuminuria induced by an anti-Nphs Ab. Thus, taking these observations into consideration, anti-Nphs Ab-induced podocytopathy is a disorder caused by an imbalance of glycosphingolipids in the cells. The expression of GM3 is crucial for maintaining a healthy kidney.

Our results showed that nephrin, GM3 and Fyn, which were originally localized in the raft fraction, shift to the non-raft fraction by anti-Nphs Ab treatment (Supplementary Fig. S4D,E). Fyn is a tyrosine kinase involved in a variety of functions including regulation of survival²⁷, cell adhesion²⁸, integrin mediated signaling^{29–31} and cytoskeletal remodeling^{32–35}. There are many reports focusing on the relationship between nephrin and cytoskeletal remodeling^{36–38}. However, our results indicated that abundant levels of GM3 in the raft fraction can inhibit the shift of nephrin and Fyn to the non-raft fraction even during anti-Nphs Ab treatment. Thus, nephrin injury caused by anti-Nphs Ab was reduced by enhanced GM3 expression in the cell membrane. This observation may indicate the mechanism by which GM3 elicits a preventive effect on albuminuria in anti-Nphs Ab-induced podocytopathy mice.

Jin et al. reported that the soluble form of vascular endothelial growth factor (VEGF) receptor (sFlt1), which is expressed on podocytes, binds GM3 enriched lipid-rafts in the cell membrane of podocyte foot processes, thereby controlling cytoskeleton reconstitution and cell adhesion via activation of nephrin and syndecan protein family members⁴. Furthermore, sFlt1 and GM3 might have a cooperative role in maintaining normal kidney function. Indeed, VEGF controls and assembles various protein functions on lipid-rafts including nephrin phosphorylation^{37,38}, cytoskeleton reconstitution³⁶ and adhesion in podocytes^{38,39}. However, except for one study suggesting GM3 is required for normal kidney function in human, which was based on immunoelectron microscopy³, there have been no further reports on this matter.

There are several reports focusing on the therapeutic effect of VPA on albuminuria. Studies on adriamycin-induced nephropathy mice, lipopolysaccharide mice and diabetic nephropathy rats^{14,15} and one involving a cohort of US veterans¹⁵ reported that VPA was particularly effective at inhibiting the progression of renal dysfunction in a group of patients with severe albuminuria. VPA acts not only as an up-regulator of *ST3GAL5* (or *St3gal5*) but also as an HDAC inhibitor. The therapeutic mechanism in these studies was presumed to involve the anti-inflammatory effect mediated by the HDAC class I inhibitory action of VPA. Moreover, other researchers have found the therapeutic effect of Trichostatin A, which exhibits HDAC class I inhibition, was more potent than VPA, although weaker in adriamycin-induced nephropathy mice^{40–42}. In this study, our observations demonstrated VPA was ineffective in preventing podocytopathy in *St3gal5*^{-/-} mice. These results clearly showed that GM3 is essential for glomerular maintenance of normal mouse kidney. Therefore, we suggest that the primary biological action of VPA related to these observations in preventing albuminuria is elevated levels of GM3 via up-regulation of *ST3GAL5*, which might be related to its HDAC inhibitory activity. Moreover, this proposal is strongly supported by our observation of anti-Nphs Ab-induced podocytopathy in *St3gal5*^{-/-} mice despite pre-administration of VPA.

This study has demonstrated the preventive mechanism mediated by GM3 using several animal and cell models. Our findings suggest glycosphingolipids, especially GM3, play a fundamental role in maintaining podocyte function (slit diaphragm stabilization, cell survival, etc.). We propose that the inhibition mechanism of albuminuria occurs via enhancement of GM3, which localizes around the nephrin transmembrane domain to inhibit changes in the conformation of nephrin caused by anti-Nphs Ab binding. Hence, the overall effect of the preventive treatment is to maintain nephrin on the cell surface, retaining its function and the integrity of the slit diaphragm, thereby sustaining the glomerular filtration barrier. These findings suggest a new therapeutic approach for podocytopathy.

Methods

See Supplementary Information for additional information.

Animal study. C57BL/6N mice (male, 7 week-old, 19–20 g) were purchased from CLEA Japan Inc. (Tokyo, Japan) and GM3 synthase gene knockout (*St3gal5*^{-/-}) mice were generated by Dr. Yamashita et al. as described previously²⁵. C57BL/6 N mice and GM3 synthase gene knockout (*St3gal5*^{-/-}) mice (male, 13 and 33 week-old, 20–25 and 27–30 g) were housed in metabolic cages under specific-pathogen-free conditions and fed a standard chow.

We previously reported an anti-mouse nephrin polyclonal antibody (anti-Nphs Ab) raised in rabbits and generated using a genetic immunization method¹⁹. Antibody from antisera was purified using nProtein A Sepharose Fast Flow (#17528001; GE Healthcare, Chicago, IL, USA). For in vivo testing, mice were first randomized into three groups: i) control group, ii) VPA treated group, (iii) anti-Nphs Ab-induced podocytopathy group, iv) VPA treated anti-Nphs Ab-induced podocytopathy group (each n = 6, respectively). To induce podocytopathy in mice, C57BL/6 and *St3gal5*^{-/-} mice were injected with a single aliquot of either 1.5 mg of anti-Nphs Ab via the tail vein. VPA was administered as 4 mM VPA in drinking water (100 mg/kg/day as human equivalent dose). This dosage is ensured safety as drugs in human)⁴³. Kidney tissues from three groups of C57BL/6 mice (groups of on day 1, 7, 14 after anti-Nphs Ab administration) were sampled and used for various analyses.

Tissue staining. Kidney tissues with p57 and periodic acid-Schiff (PAS) staining was assessed as previously described^{44,45}. Glomerulosclerosis was graded quantitatively by the percentage of glomerular tuft area involvement as follows¹⁹: score 0, no sclerosis; score 1, <25%; score 2, 25–50%; score 3 50–75%; score 4, 75–100%. Global sclerosis means glomeruli with more than 75% tuft area scleroses, which is a score of 4. Immunofluorescence staining of nephrin and GM3 were carried out using frozen sections of mouse kidney tissues with various antibodies. Pathological images were visualized by optical microscopy (BX51; Olympus, Tokyo, Japan) and analyzed by ImageJ software (<https://imagej.nih.gov/ij/>). Fluorescence images were obtained using a confocal laser-microscope (LSM710; Carl Zeiss, Oberkochen, Germany) and analyzed by ZEN imaging software (Carl Zeiss).

Glycosphingolipid-glycan preparation by glycoblotting method. Approximately 1×10^6 cells were suspended in 200 μ L of PBS and homogenized using an Ultrasonic Homogenizer. Ethanol precipitation was carried out by incubation at -30°C for 16 h. The cellular proteinaceous pellet and supernatant/lipid fractions were separated by centrifugation. Cellular pellets were dissolved in 100 μ L of water and the protein concentration was measured using BCA protein assay kit (#23227; Thermo Fisher Scientific, Waltham, MA, USA). To release intact glycosphingolipid-glycans, the supernatant/lipid fractions corresponding to 400 μ g protein were dried to remove ethanol and then resuspended in 45 μ L of 50 mM acetate buffer, pH 5.5, containing 0.2% Triton X-100. Enzymatic digestion was performed by the addition of 5 μ L endoglycosamidase I (EGCase I) followed by incubation at 37°C for 16 h²³. To take account of free oligosaccharide (fOSs) contamination in the lipid fractions, non-enzymatic digestion samples were prepared as negative controls²¹. The kidney tissues were homogenized in 100 μ L PBS(-) using an beads crusher (TAITEC, Saitama, Japan). The method for protein quantification and intact glycosphingolipid-glycan release were the same as procedure described above.

Glycosphingolipid-glycan purification for MALDI-TOF MS analysis. Released glycosphingolipid-glycans were subjected to a glycoblotting procedure as previously described²⁰. In brief, EGCase digested samples (25 μ L), using involving an internal standard of Neu5Ac2Gal2GlcNAc2 + Man3GlcNAc1 (A2GN1, 10 pmol), were captured on BlotGlyco[®] beads (5 mg; Sumitomo Bakelite Co., Ltd, Tokyo, Japan). Unreacted hydrazide groups on beads were capped with acetyl groups by treatment with 10% acetic anhydride in methanol. To protect carboxy groups of sialic acids, methyl esterification was performed with 100 mM 3-methyl-1-*p*-tolyltriazene in dioxane on a solid-phase. Next, these methyl esterified glycans were released and labeled with aminooxy-functionalized tryptophanylarginine methyl ester (aoWR) via a transamination reaction. Excessive aoWR reagent was removed by solid-phase extraction using a HILIC μ Elution plate (#186002780; Waters, Milford, MA, USA). Purified glycan solutions were mixed with 2,5-dihydroxybenzoic acid (10 mg/mL in 30% ACN) and subsequently subjected to MALDI-TOF MS analysis as previously described²². Briefly, all measurements were performed using an Ultraflex II TOF/TOF mass spectrometer equipped with a reflector and controlled by the FlexControl 3.0 software package (Bruker Daltonics, Bremen, Germany) according to general protocols. All spectra were obtained in reflectron mode with an acceleration voltage of 25 kV, a reflector voltage of 26.3 kV, and a pulsed ion extraction of 160 ns in positive ion mode. Masses were annotated using the FlexAnalysis 3.0 software package. SphinGOMAP (<http://www.sphingomap.org/>) online databases were used for structural identification of GSL-glycans. Absolute quantification was performed by comparative analyses between the areas of the MS signals derived from each GSL-glycan and a known amount of the internal standard (A2GN1).

Glycosphingolipid extraction and high-performance TLC analysis. Glycosphingolipid extraction was performed as described previously^{46,47}. In brief, 2×10^8 cells were harvested using a rubber scraper and washed with PBS. Gangliosides from cells were extracted by sonication 4 times in isopropanol/hexane/water (IP/H/W) (55:25:20, by volume). Extracts were combined, evaporated and dissolved in 6 volumes of chloroform/methanol (CM) (2:1, by volume) and water was added to achieve chloroform/methanol/water (CMW) (4:2:1, by volume). After shaking, the mixture was allowed to separate into upper and lower phases. The upper phases containing glycosphingolipid, which partitioned according to the Folch procedure, were combined and evaporated. Dried upper phases were solubilized in distilled water and the resultant solution was applied to a Sep-Pak Plus C18 cartridge (#WAT020515; Waters, Milford, MA, USA) for desalting. Purified glycosphingolipids were developed on high-performance TLC (HPTLC) plates (#1.05641.0001; Merck, Darmstadt, Germany) with a solvent system consisting of chloroform/methanol/0.2% aqueous CaCl_2 (CMW) (55:45:10, by volume), and visualized by spraying with 0.5% orcinol in 1 M sulfuric acid.

Statistical analysis. Data were analyzed as the mean \pm SEM. Statistical comparisons between two groups were evaluated by Mann–Whitney's U-test. Multiple-group comparisons were evaluated using 1-way ANOVA followed by Tukey's test. Statistical analysis was performed by StatFlex Ver.7 (Artech, Osaka, Japan). A *P*-value of less than 0.05 was considered statistically significant.

Study approval. All animal experiments were approved by the Ethical Review Committee for Animal Experiments of Kitasato University School of Medicine (#2017-182, #2018-006, #2019-072, #2020-016) and Azabu University of Veterinary Medicine (#201204-2). DNA studies were approved by the Ethical Review Committee for Recombinant DNA Experiments of Kitasato University School of Medicine (#3837). All experiments were performed in accordance with relevant guidelines and regulations and the study is reported in accordance with ARRIVE guidelines.

Data availability

The data generated during this study are available on reasonable request.

Received: 23 May 2022; Accepted: 12 September 2022

Published online: 26 September 2022

References

- Ahn, W. & Bombardieri, A. S. Approach to diagnosis and management of primary glomerular diseases due to podocytopathies in adults: Core curriculum 2020. *Am. J. Kidney Dis.* **75**, 955–964. <https://doi.org/10.1053/j.ajkd.2019.12.019> (2020).
- Savas, B., Astarita, G., Aureli, M., Sahali, D. & Ollero, M. Gangliosides in podocyte biology and disease. *Int. J. Mol. Sci.* **21**, 9645. <https://doi.org/10.3390/ijms21249645> (2020).
- Kaneko, T. *et al.* Histochemical and immunoelectron microscopic analysis of ganglioside GM3 in human kidney. *Clin. Exp. Nephrol.* **19**, 403–410. <https://doi.org/10.1007/s10157-014-1003-0> (2015).
- Jin, J. *et al.* Soluble FLT1 binds lipid microdomains in podocytes to control cell morphology and glomerular barrier function. *Cell* **151**, 384–399. <https://doi.org/10.1016/j.cell.2012.08.037> (2012).
- Naito, S. *et al.* Decreased GM3 correlates with proteinuria in minimal change nephrotic syndrome and focal segmental glomerulosclerosis. *Clin. Exp. Nephrol.* <https://doi.org/10.1007/s10157-022-02249-2> (2022).
- Hakomori, S. I. Structure and function of glycosphingolipids and sphingolipids: Recollections and future trends. *Bba-Gen Subjects* **1780**, 325–346. <https://doi.org/10.1016/j.bbagen.2007.08.015> (2008).
- Bremer, E. G., Schlessinger, J. & Hakomori, S. Ganglioside-mediated modulation of cell growth. Specific effects of GM3 on tyrosine phosphorylation of the epidermal growth factor receptor. *J. Biol. Chem.* **261**, 2434–2440 (1986).
- Yoon, S. J., Nakayama, K., Hikita, T., Handa, K. & Hakomori, S. I. Epidermal growth factor receptor tyrosine kinase is modulated by GM3 interaction with N-linked GlcNAc termini of the receptor. *Proc. Natl. Acad. Sci. USA* **103**, 18987–18991. <https://doi.org/10.1073/pnas.0609281103> (2006).
- Kabayama, K. *et al.* Dissociation of the insulin receptor and caveolin-1 complex by ganglioside GM3 in the state of insulin resistance. *Proc. Natl. Acad. Sci. USA* **104**, 13678–13683. <https://doi.org/10.1073/pnas.0703650104> (2007).
- Kawashima, N., Yoon, S. J., Itoh, K. & Nakayama, K. Tyrosine kinase activity of epidermal growth factor receptor is regulated by GM3 binding through carbohydrate to carbohydrate interactions. *J. Biol. Chem.* **284**, 6147–6155. <https://doi.org/10.1074/jbc.M808171200> (2009).
- Kawashita, E. *et al.* Abnormal production of macrophage inflammatory protein-1 α by microglial cell lines derived from neonatal brains of Sandhoff disease model mice. *J. Neurochem.* **109**, 1215–1224. <https://doi.org/10.1111/j.1471-4159.2009.06041.x> (2009).
- Kawashima, N., Tsuji, D., Okuda, T., Itoh, K. & Nakayama, K. Mechanism of abnormal growth in astrocytes derived from a mouse model of GM2 gangliosidosis. *J. Neurochem.* **111**, 1031–1041. <https://doi.org/10.1111/j.1471-4159.2009.06391.x> (2009).
- Kawashima, N., Nishimiya, Y., Takahata, S. & Nakayama, K. I. Induction of glycosphingolipid GM3 expression by valproic acid suppresses cancer cell growth. *J. Biol. Chem.* **291**, 21424–21433. <https://doi.org/10.1074/jbc.M116.751503> (2016).
- Van Beneden, K. *et al.* Valproic acid attenuates proteinuria and kidney injury. *J. Am. Soc. Nephrol.* **22**, 1863–1875. <https://doi.org/10.1681/ASN.2010111196> (2011).
- Inoue, K. *et al.* Podocyte histone deacetylase activity regulates murine and human glomerular diseases. *J. Clin. Invest.* **129**, 1295–1313. <https://doi.org/10.1172/JCI124030> (2019).
- Kwon, H. Y. *et al.* Valproic acid-mediated transcriptional regulation of human GM3 synthase (hST3Gal V) in SK-N-BE(2)-C human neuroblastoma cells. *Acta Pharmacol. Sin.* **29**, 999–1005. <https://doi.org/10.1111/j.1745-7254.2008.00847.x> (2008).
- Song, N. *et al.* Transcriptional activation of human GM3 synthase (hST3Gal V) gene by valproic acid in ARPE-19 human retinal pigment epithelial cells. *BMB Rep.* **44**, 405–409. <https://doi.org/10.5483/BMBRep.2011.44.6.405> (2011).
- Watts, A. J. B. *et al.* Discovery of autoantibodies targeting nephrin in minimal change disease supports a novel autoimmune etiology. *J. Am. Soc. Nephrol.* **33**, 238–252. <https://doi.org/10.1681/ASN.2021060794> (2022).
- Takeuchi, K. *et al.* New anti-nephrin antibody mediated podocyte injury model using a C57BL/6 mouse strain. *Nephron* **138**, 71–87. <https://doi.org/10.1159/000479935> (2018).
- Furukawa, J. *et al.* Comprehensive approach to structural and functional glycomics based on chemoselective glycoblotting and sequential tag conversion. *Anal. Chem.* **80**, 1094–1101. <https://doi.org/10.1021/ac702124d> (2008).
- Fujitani, N. *et al.* Qualitative and quantitative cellular glycomics of glycosphingolipids based on rhodococcal endoglycosylceramidase-assisted glycan cleavage, glycoblotting-assisted sample preparation, and matrix-assisted laser desorption/ionization tandem time-of-flight mass spectrometry analysis. *J. Biol. Chem.* **286**, 41669–41679. <https://doi.org/10.1074/jbc.M111.301796> (2011).
- Furukawa, J. *et al.* Quantitative GSL-glycome analysis of human whole serum based on an EGCase digestion and glycoblotting method. *J. Lipid Res.* **56**, 2399–2407. <https://doi.org/10.1194/jlr.D062083> (2015).
- Ishibashi, Y. *et al.* A novel endoglycosylceramidase hydrolyzes oligogalactosylceramides to produce galactooligosaccharides and ceramides. *J. Biol. Chem.* **282**, 11386–11396. <https://doi.org/10.1074/jbc.M608445200> (2007).
- Fornoni, A., Merscher, S. & Kopp, J. B. Lipid biology of the podocyte—new perspectives offer new opportunities. *Nat. Rev. Nephrol.* **10**, 379–388. <https://doi.org/10.1038/nrneph.2014.87> (2014).
- Yamashita, T. *et al.* Enhanced insulin sensitivity in mice lacking ganglioside GM3. *Proc. Natl. Acad. Sci. USA* **100**, 3445–3449. <https://doi.org/10.1073/pnas.0635898100> (2003).
- Hakomori, S. The glycosynapse (vol 99, pg 225, 2002). *Proc. Natl. Acad. Sci. USA* **99**, 3356–3356. <https://doi.org/10.1073/pnas.062024099> (2002).
- Greka, A. & Mundel, P. Cell biology and pathology of podocytes. *Annu. Rev. Physiol.* **74**, 299–323. <https://doi.org/10.1146/annurev-physiol-020911-153238> (2012).
- Verma, R. *et al.* Fyn binds to and phosphorylates the kidney slit diaphragm component Nephrin. *J. Biol. Chem.* **278**, 20716–20723. <https://doi.org/10.1074/jbc.M301689200> (2003).
- Wary, K. K., Mariotti, A., Zurzolo, C. & Giancotti, F. G. A requirement for caveolin-1 and associated kinase Fyn in integrin signaling and anchorage-dependent cell growth. *Cell* **94**, 625–634. [https://doi.org/10.1016/s0092-8674\(00\)81604-9](https://doi.org/10.1016/s0092-8674(00)81604-9) (1998).
- Chapman, H. A., Wei, Y., Simon, D. I. & Waltz, D. A. Role of urokinase receptor and caveolin in regulation of integrin signaling. *Thromb. Haemost.* **82**, 291–297 (1999).

31. Dlugos, C. P. *et al.* Nephron signaling results in integrin beta1 activation. *J. Am. Soc. Nephrol.* **30**, 1006–1019. <https://doi.org/10.1681/ASN.2018040362> (2019).
32. Thomas, S. M., Soriano, P. & Imamoto, A. Specific and redundant roles of Src and Fyn in organizing the cytoskeleton. *Nature* **376**, 267–271. <https://doi.org/10.1038/376267a0> (1995).
33. Harita, Y. *et al.* Neph1, a component of the kidney slit diaphragm, is tyrosine-phosphorylated by the Src family tyrosine kinase and modulates intracellular signaling by binding to Grb2. *J. Biol. Chem.* **283**, 9177–9186. <https://doi.org/10.1074/jbc.M707247200> (2008).
34. Lv, Z. *et al.* Fyn mediates high glucose-induced actin cytoskeleton reorganization of podocytes via promoting ROCK activation in vitro. *J. Diabetes Res.* **2016**, 5671803. <https://doi.org/10.1155/2016/5671803> (2016).
35. Kawachi, H. & Fukusumi, Y. New insight into podocyte slit diaphragm, a therapeutic target of proteinuria. *Clin. Exp. Nephrol.* **24**, 193–204. <https://doi.org/10.1007/s10157-020-01854-3> (2020).
36. Jones, N. *et al.* Nck adaptor proteins link nephrin to the actin cytoskeleton of kidney podocytes. *Nature* **440**, 818–823. <https://doi.org/10.1038/nature04662> (2006).
37. Carney, E. F. Podocyte biology: Phosphorylation preserves podocytes. *Nat. Rev. Nephrol.* **12**, 197. <https://doi.org/10.1038/nrneph.2016.17> (2016).
38. Martin, C. E. & Jones, N. Nephron signaling in the podocyte: An updated view of signal regulation at the slit diaphragm and beyond. *Front. Endocrinol.* **9**, 302. <https://doi.org/10.3389/fendo.2018.00302> (2018).
39. Lennon, R., Randles, M. J. & Humphries, M. J. The importance of podocyte adhesion for a healthy glomerulus. *Front. Endocrinol.* **5**, 160. <https://doi.org/10.3389/fendo.2014.00160> (2014).
40. Phiel, C. J. *et al.* Histone deacetylase is a direct target of valproic acid, a potent anticonvulsant, mood stabilizer, and teratogen. *J. Biol. Chem.* **276**, 36734–36741. <https://doi.org/10.1074/jbc.M101287200> (2001).
41. Kramer, O. H. *et al.* The histone deacetylase inhibitor valproic acid selectively induces proteasomal degradation of HDAC2. *EMBO J.* **22**, 3411–3420. <https://doi.org/10.1093/emboj/cdg315> (2003).
42. Garpnis, N. *et al.* Targeting histone deacetylases in malignant melanoma: A future therapeutic agent or just great expectations?. *Anticancer Res.* **37**, 5355–5362. <https://doi.org/10.21873/anticancer.11961> (2017).
43. Tremolizzo, L. *et al.* An epigenetic mouse model for molecular and behavioral neuropathologies related to schizophrenia vulnerability. *Proc. Natl. Acad. Sci. USA* **99**, 17095–17100. <https://doi.org/10.1073/pnas.262658999> (2002).
44. Suzuki, T., Eng, D. G., McClelland, A. D., Pippin, J. W. & Shankland, S. J. Cells of NG2 lineage increase in glomeruli of mice following podocyte depletion. *Am. J. Physiol. Renal Physiol.* **315**, F1449–F1464. <https://doi.org/10.1152/ajprenal.00118.2018> (2018).
45. Hassan, H. *et al.* Essential role of X-box binding protein-1 during endoplasmic reticulum stress in podocytes. *J. Am. Soc. Nephrol.* **27**, 1055–1065. <https://doi.org/10.1681/ASN.2015020191> (2016).
46. Liang, Y. J. *et al.* Differential expression profiles of glycosphingolipids in human breast cancer stem cells vs. cancer non-stem cells. *Proc. Natl. Acad. Sci. USA* **110**, 4968–4973. <https://doi.org/10.1073/pnas.1302825110> (2013).
47. Kannagi, R., Nudelman, E., Levery, S. B. & Hakomori, S. A series of human erythrocyte glycosphingolipids reacting to the monoclonal antibody directed to a developmentally regulated antigen SSEA-1. *J. Biol. Chem.* **257**, 14865–14874 (1982).

Acknowledgements

We thank Dr. Itakura M. for help of anti-nephron antibody (anti-cNphs Ab) production, Ms. Ishigaki N. for help with tissue staining, Ms. Yamaguchi N. for the kind gift of *St3gal5^{-/-}* mice, Dr. Shankland S.J. for the kind gift of mouse podocytes and Dr. Nakamura K. for analysis of high-performance thin layer chromatography.

Author contributions

N.K. and K.N. conceived, designed and N.K., S.N. and K.N. supervised the study. N.K., H.H. and M.N. wrote and N.K., S.N. and K.N. edited the manuscript. N.K., S.N., Y.T. and T.Y. performed in vivo tests and histological studies, N.K. and M.N. performed in vitro experiments. H.H., J.F. and N.I. performed MALDI-TOF/MS analysis. All authors contributed to the review and approval of the final manuscript.

Funding

This study was supported by a grant from the Suzuken Memorial Foundation (16–061 to NK), JSPS KAKENHI (17K09709, 20K08615 to NK, 18K08249 to SN), and the Cooperative Research Program of “Network Joint Research Center for Materials and Devices” (20201013 to NK).

Competing interests

The authors declare no competing interests.

Additional information

Supplementary Information The online version contains supplementary material available at <https://doi.org/10.1038/s41598-022-20265-w>.

Correspondence and requests for materials should be addressed to N.K.

Reprints and permissions information is available at www.nature.com/reprints.

Publisher’s note Springer Nature remains neutral with regard to jurisdictional claims in published maps and institutional affiliations.



Open Access This article is licensed under a Creative Commons Attribution 4.0 International License, which permits use, sharing, adaptation, distribution and reproduction in any medium or format, as long as you give appropriate credit to the original author(s) and the source, provide a link to the Creative Commons licence, and indicate if changes were made. The images or other third party material in this article are included in the article’s Creative Commons licence, unless indicated otherwise in a credit line to the material. If material is not included in the article’s Creative Commons licence and your intended use is not permitted by statutory regulation or exceeds the permitted use, you will need to obtain permission directly from the copyright holder. To view a copy of this licence, visit <http://creativecommons.org/licenses/by/4.0/>.

© The Author(s) 2022